Prophage-encoded small protein YqaH counteracts the activities of the replication initiator DnaA in Bacillus subtilis

Magali Ventroux, Marie-Francoise Noirot-Gros

MICROBIOLOGY

MICROBIOLOGY SOCIETY

OPEN ACCESS

Prophage-encoded small protein YqaH counteracts the activities of the replication initiator DnaA in *Bacillus subtilis*

Magali Ventroux and Marie-Francoise Noirot-Gros*
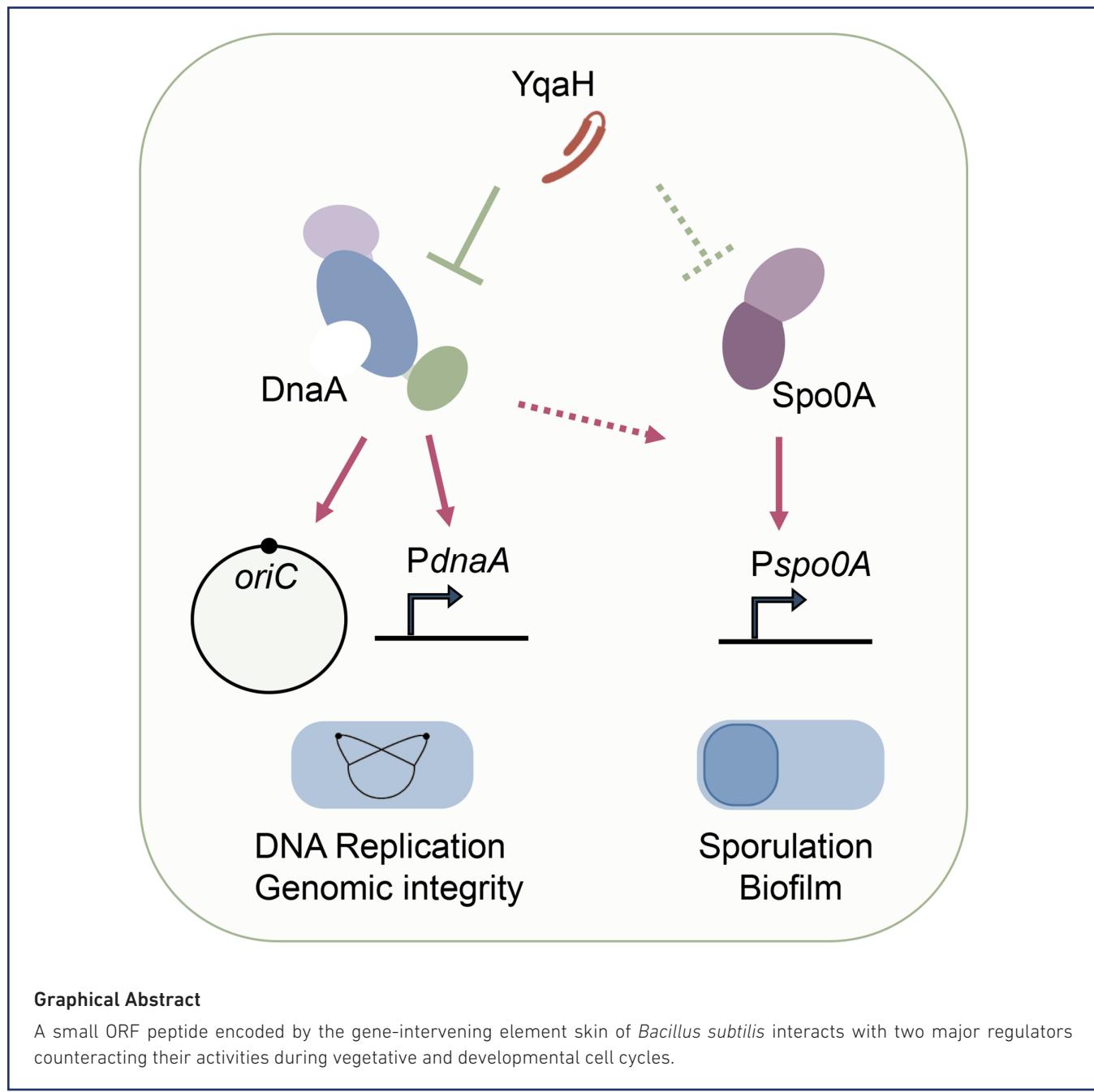
Graphical Abstract

A small ORF peptide encoded by the gene-intervening element skin of *Bacillus subtilis* interacts with two major regulators counteracting their activities during vegetative and developmental cell cycles.

Abstract

Bacterial genomes harbour cryptic prophages that are mostly transcriptionally silent with many unannotated genes. Still, cryptic prophages may contribute to their host fitness and phenotypes. In *Bacillus subtilis,* the *yqaF-yqaN* operon belongs to the prophage element *skin*, and is tightly repressed by the Xre-like repressor SknR. This operon contains several small ORFs (smORFs) potentially encoding small-sized proteins. The smORF-encoded peptide YqaH was previously reported to bind to the replication initiator DnaA. Here, using a yeast two-hybrid assay, we found that YqaH binds to the DNA binding domain IV of DnaA and interacts with Spo0A, a master regulator of sporulation. We isolated single amino acid substitutions in YqaH that abolished the interaction with DnaA but not with Spo0A. Then, using a plasmid-based inducible system to overexpress *yqaH* WT and mutant derivatives, we studied in *B. subtilis* the phenotypes associated with the specific loss-of-interaction with DnaA (DnaA_LOI). We found that expression of *yqaH* carrying DnaA_LOI mutations abolished the deleterious effects of *yqaH* WT expression on chromosome segregation, replication initiation and DnaA-regulated transcription. When YqaH was induced after vegetative growth, DnaA_LOI mutations abolished the drastic effects of YqaH WT on sporulation and biofilm formation. Thus, YqaH inhibits replication, sporulation and biofilm formation mainly by antagonizing DnaA in a manner that is independent of the cell cycle checkpoint Sda.

INTRODUCTION

small ORF (smORF)-encoded peptides (SEP) have emerged as a new class of small proteins widespread in both eukaryotic and prokaryotic genomes [1–5]. Due to their small size (for the smallest <30 aa or microproteins up to 100 aa) SEPs have often been overlooked during genome annotation. However, with advanced computation and ribosome profiling-based biochemical methods, small proteins are now more widely identified and some have been functionally characterized [4, 6–10]. Growing evidence indicates that smORFs often encode bioactive peptides [6, 11]. However, their contribution to cellular functions remains largely unexplored.

Small proteins act as regulators of diverse cellular processes in eukaryotes [12]. In plants, characterized small proteins regulate transcription factors by sequestering them into non-functional states, preventing DNA binding or transcriptional activation [13, 14]. In *Drosophila melanogaster,* smORFs represent about 5% of the transcriptome and play an important role in controlling *Drosophila* development by triggering post-translational processing of transcriptional regulators [1, 15]. In humans, SEPs have been discovered with specific subcellular localization, suggesting they can fulfil biological functions [16]. For instance, a 69 aa long peptide, MRI-2, has been described to play a role in stimulating DNA repair through binding to the DNA end-binding protein complex Ku [17]. smORFs represent about 2% of the genome of *Saccharomyces cerevisiae* [18]. Their function remains largely elusive but few have been identified to play regulatory roles in diverse physiological processes such as iron homeostasis [19] or DNA synthesis [18, 20, 21]. Genomic analysis of *S. cerevisiae* revealed that a substantial fraction of smORFs are conserved in other eukaryotes even as phylogenetically distantly related as humans, thus emphasizing their biological significance [22].

In prokaryotes, small proteins are encoded by 10–20% of sRNA on average, and are often species-specific [10, 23–26]. SEPs with characterized functions are involved in various cellular processes [5]. In *Pseudomonas aeruginosa*, PtrA (63 aa long) and PtrB (59 aa long) repress the type III secretion system in response to DNA stress [27, 28]. In *Escherichia coli*, the 43 aa long peptide SgrT interferes with the PTS glucose transport system, allowing cells to utilize alternative non-PTS carbon sources to rapidly adapt to environmental changes in nutrient availability [29]. In *Bacillus subtilis*, SEPs participate in regulating cell division and stress responses [30–32]. A compelling example is the recently characterized developmental regulator MciZ (mother cell inhibitor of FtsZ), a 40 aa long peptide which prevents cytokinesis in the mother cell during sporulation [33, 34]. About 20% of the total core protein of the mature spores of *B. subtilis* is composed of the small acid-soluble spore proteins (SASPs) playing an important role in protecting DNA in the dormant spores [35, 36]. Notably, several smORFs identified in intergenic regions were reported to be expressed during sporulation [32]. The sporulation inhibitor *sda* encodes a 52 aa long protein, which acts as a checkpoint system coordinating DNA replication with sporulation initiation [37–39]. Sda binds to the primary sporulation kinase KinA, preventing its activation as well as the subsequent phosphorelay-mediated activation of the master sporulation regulator Spo0A

Fig. 1. YqaH interacts with DnaA and Spo0A. (a) SknR transcriptionally represses the yqaF–yqaN operon of the Skin element. (b, c) Yeast two-hybrid interaction assay. Haploid yeast strains expressing the *yqaH*, *dnaA* and *yabA* gene or DNA fragments fused to the BD or AD domains of GAL4 are separately introduced into haploid yeast strains. Binary interactions are tested by the ability of diploids to grow onto selective media. (d) DnaA interaction with YqaH and regulators. Schematic representation of the architecture of the four functional domains of DnaA with associated functions as illustrated by colours. Numbers refer to amino acid boundaries. The binding of negative regulators to their targeted DnaA functional domain is illustrated accordingly. The YqaH interacting domains of DnaA with associated yeast two-hybrid interacting phenotypes (IP) are indicated. (+) and (-) refer to growth or absence of growth on selective media, reflecting an interacting or loss-of-interaction phenotype, respectively.

[38, 40]. By linking DNA replication to a phosphorylation-dependent signalling cascade that triggers cellular development, this system illustrates an important biological role played by an SEP in blocking sporulation in response to DNA stress in *Bacillus* [40].

Small proteins encoded by phage or by prophage-like regions of bacterial genomes can hijack the host cellular machineries, as part of a strategy to shift host resources toward the production of viral progeny [41–43]. The bacteriophage T7 gene 2 encodes the 64 aa long gp2 protein essential for infecting *E. coli*. Studies of its biological role revealed that gp2 inhibits bacterial transcription by binding to RNA polymerase (RNAP), promoting a host-to-viral RNAP switch [44, 45]. Another example is the 52 aa long protein ORF104 of phage 77 infecting *Staphylococcus aureus*. ORF104 is able to interfere with the host chromosome replication by binding to the ATPase domain of the helicase loader protein DnaI, thus preventing loading of the DNA helicase DnaC [46, 47].

In bacteria, DNA replication is initiated by the conserved initiator protein DnaA that assembles to the chromosomal replication origin to elicit local DNA strand opening [48–51]. This step triggers the coordinated assembly of the proteins that will further build a functional replication fork, from the DNA helicase, unwinding the DNA duplex, to the many components of the replisome that form the replication machinery [52]. In addition to its initiator activity, DnaA acts as a transcription factor repressing or activating genes [53–55]. The activity of the initiator DnaA is tightly controlled to coordinate chromosomal replication initiation with other cellular processes during the bacterial cell cycle [56, 57]. Part of this control is mediated by protein–protein interactions and involves various protein regulators that bind DnaA and affect its activity [58–62]. In *B. subtilis*, four proteins, SirA, Soj, DnaD and YabA, have been identified to regulate DnaA activity or its assembly at *oriC* through direct interaction [58, 63–65].

Phage SEPs targeting essential functions for bacterial survival are regarded as promising antimicrobial peptides, and have ignited a strong interest in their identification and characterization [46, 47]. The phage-like element *skin* of *B. subtilis* encodes about 60 proteins. The *skin* element is repressed under most physiological conditions [66], silenced by the *skin* repressor SknR (Fig. 1a) [67]. The excision of *skin* from the genome is mediated by the self-encoded site-specific recombinase CisA and restores the integrity of the *sigK* gene encoding the late sporulation factor σ^K [68]. Among the *skin* ORFs, *yqaH* encodes the 85 aa long polypeptide YqaH previously identified to bind to the replication initiator protein DnaA in a yeast two-hybrid genomic screen [69, 70]. When *yqaH* is overexpressed, *Bacillus* cells exhibit aberrant nucleoid morphological defects suggestive of replication deficiency [67]. In this study, we further characterized the function of YqaH in antagonizing DnaA activities. In addition, we found that YqaH also interacts with the master regulator Spo0A involved in developmental transitions to sporulation and biofilm formation [71]. As with DnaA, Spo0A is a DNA-binding protein, which, in its activated phosphorylated form (Spo0A-P), controls the expression of numerous genes during the early stages of sporulation [72]. To better understand the biological role of this smORF in *B. subtilis* we performed a functional dissection of YqaH. Using a reverse yeast two-hybrid system, we selected *yqaH* alleles that selectively disrupted the YqaH/DnaA complex. This approach allowed us to link specific DnaA loss-of-interaction with loss-of-function phenotypes related to replicative stress. Interestingly, it also highlighted an intricate role of both DnaA and Spo0A in YqaH-mediated sporulation phenotypes.

METHODS

Strains, plasmids and primers

Experiments were performed in *B. subtilis* strains 168 or BSBA1 (168 trpC2). *S. cerevisiae* PJ69-4a or α strains were used for yeast two-hybrid experiments [73]. All strains are listed in Table S1A (available in the onlive version of this article). *E. coli* strain DH10B [74] was used as a cloning host. Plasmid constructs are listed in Table S1B. Primers are listed in Table S2. Sequences of interest cloned or mutated in this study were verified by DNA sequencing.

Bacteria growth

Experiments were conducted at 37 °C in LB medium containing the necessary antibiotics such as ampicillin, 100 µg ml⁻¹ (in *E. coli*); spectinomycin, 60 µg ml⁻¹; kanamycin, 5 µg ml⁻¹; chloramphenicol, 5 µg ml⁻¹ or erythromycin, 1 µg ml⁻¹ associated with lincomycin, 25 µg ml⁻¹ (for *B. subtilis*). *B. subtilis* strains containing pDG148 and pDG148-*yqaH* plasmids were grown overnight in LB containing kanamycin. To investigate the effect of *yqaH* expression during exponential phase growth, ON cultures were diluted at OD_{600} of 0.01 onto fresh LB (+Kn) media and grown to mid-exponential phase (OD_{600} 0.3–0.4). The cultures were then further diluted in LB (+Kn) media containing 0.5 mM IPTG at OD_{600} of 0.01 and 200 µl of cultures were then transferred to a 96-well microplate reader to monitor OD_{600} at 37 °C for 18 h.

Strain constructions

yqaH overexpression

The *yqaH* wild type (WT) and mutated gene derivatives were PCR-amplified using the yqaH-HindIII-RBS-F/pYqaH-R primer pair and inserted in plasmid pDG148 between *Hind*III and *Sal*I restriction sites to place *yqaH* under control of the IPTG-inducible *Pspac* promoter [75]. The plasmid constructs were then extracted from *E. coli* and transformed into *B. subtilis*. To assess expression of YqaH variants, YqaH WT and mutated proteins were expressed as 3Flag-fusion proteins.
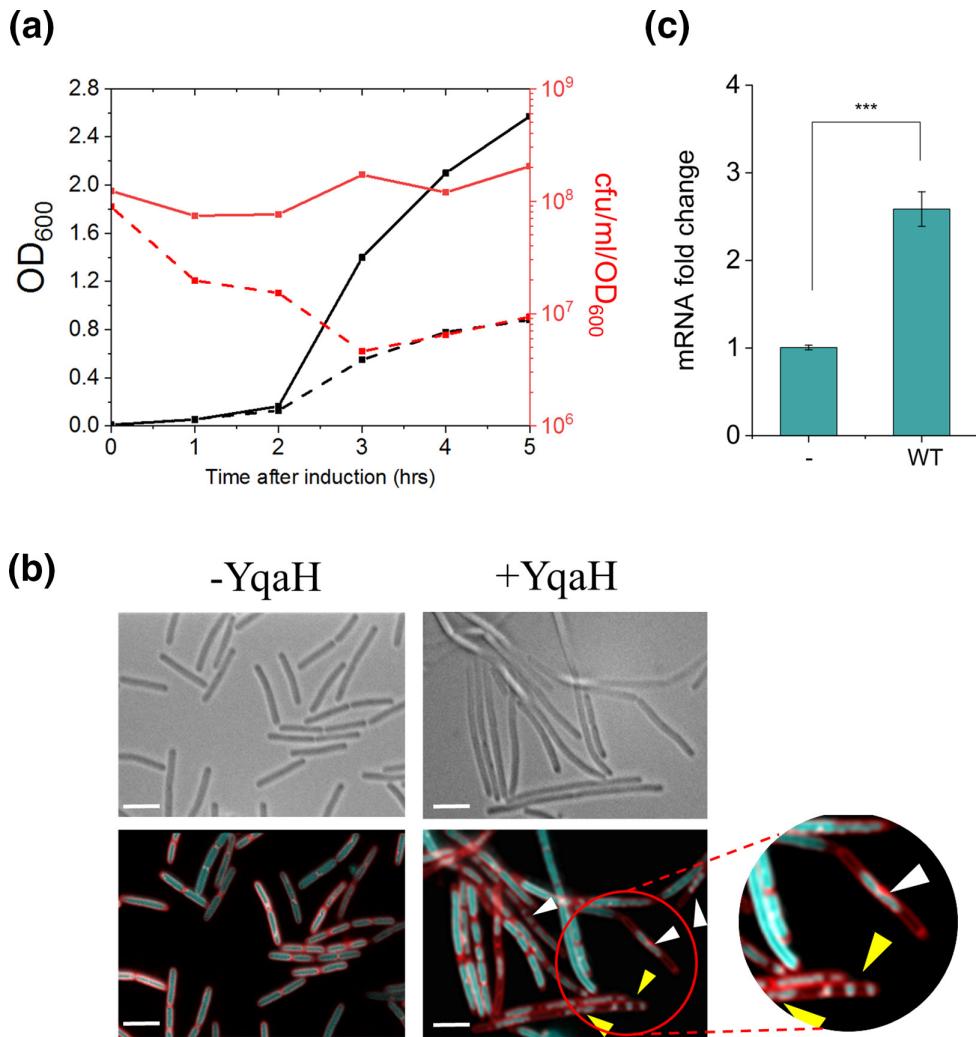
Fig. 2. YqaH triggers *dnaA*-related phenotypes. (a) Effect of *yqaH* expression on growth. Cells carrying plasmids pDG148 (control, plain lines) or pDG148-yqaH (dashed lines) were examined in the presence of IPTG (0.5 mM) over 5 h. Growth was monitored either by OD_{600} (black) or by cell viability, measured as the number of colony forming units per millilitre, normalized by OD_{600} (red). (b) Nucleoid morphological defects. Samples of living cells were examined by bright-field (above) and fluorescence microscopy (below) after staining with FM4-64 (membrane dye, false-coloured in red) and DAPI (DNA dye, false-coloured in blue). White and yellow arrows indicate guillotined chromosomes resulting from septal closing over nucleoids and aberrant nucleoid segregation patterns, respectively, and a typical example of chromosomal segregation defects is magnified. Bars, 5 μm. (c) YqaH affects *dnaA* expression. Cells harbouring either pDG148 or pDG148-yqaH were grown in LB in the presence of IPTG. RNAs from exponentially grown cells (OD_{600} 0.3) were extracted and expression levels of *dnaA* were monitored by qPCR in the presence (+) or absence (-) of YqaH. Data are presented as mean±SE; $n \geq 16$ from two independent experiments and three biological replicates per experiment. ***$P<0.001$ (*t*-test).

Yeast two–hybrid plasmid constructs

Genes encoding full size YqaH, Spo0A, YabA and DnaA were translationally fused to the activating domain (AD) or the binding domain (BD) of the transcriptional factor Gal4 by cloning into pGAD and pGBDU vectors, respectively [73]. DNA fragments were amplified by PCR using appropriate primer sets (Table S2), double digested by *Eco*RI and *Sal*I and ligated to the corresponding pGAD or pGBDU linearized vector to generate a translational fusion with Gal4-AD or BD domains. pGAD- and pGBDU- plasmid derivatives were selected onto SD media lacking leucine (SD-L) or uracyl (SD-U), respectively [73]. Plasmid constructs were first transformed into *E. coli* prior to be introduced in the haploid yeast strain PJ69-4α (pGAD-derivatives) or PJ69-4a (pGBDU-derivatives). Truncated *dnaA* fragments (boundaries as illustrated in Fig. 1d) were translationally fused to the AD of Gal4 by gap repair recombination in yeast [76]. DNA fragments were amplified by PCR using appropriate primer sets (Table S2) to generate 50 bp of flanking homology with the linearized recipient vector pGAD on both sides of the *dnaA* fragments. PJ69-4α was co-transformed with the PCR fragments containing the truncated *dnaA* domains and linearized pGAD to give rise to pGAD-truncated *dnaA* fusions by *in vivo* recombination.

Sporulation conditions

Sporulation of *B. subtilis* was induced by nutrient limitation and re-suspension in Sterlini–Mandelstam medium (SM) [77]. The beginning of sporulation (t_0) is defined as the moment of re-suspension of the cells in SM medium. To study the effects of *yqaH* overexpression on *B. subtilis* sporulation, ON cultures of strains containing the pDG148 constructions were diluted in CH medium at a starting OD_{600} of 0.05. When cultures reached an OD_{600} of 1, cells were re-suspended in an equivalent volume of SM medium supplemented with 0.5 mM IPTG (t_0). To monitor sporulation efficiency, cells were collected at different times after sporulation induction (t_0) until t_6 (6 h after induction, defined as a stage of production of mature spores) and t_{18}. Asymmetric septa and spores were enumerated ($n \geq 500$ cells) by microscopic observations from all samples.

Yeast two-hybrid assay

The yeast two-hybrid assays were performed as described [69, 70, 78]. PJ69-4a and α haploid yeast strains transformed by pGAD- and pGBDU- plasmid derivatives were mixed onto YEPD-rich media plates to allow formation of diploids. Diploids containing both pGAD- and pGBDU-type plasmids were then selected on SD-LU and interacting phenotypes were monitored by the ability of diploids to grow on SD-LUHA medium further lacking histidine (H) or adenine (A).

Generation of loss of interaction (LOI) mutation

YqaH DnaA_LOI mutants were identified using a yeast two-hybrid-based assay as described elsewhere [58, 78–80]. Random mutagenesis of the targeted genes was achieved by PCR amplification under mutagenic conditions that promote fewer than one mis-incorporation per amplification cycle [58]. For *yqaH*, a library of mutated pGAD-*yqaH** was constructed by gap-repair recombination into yeast (PJ69–4α strain). About 1000 individual transformants were organized in 96-well format on plates containing a defined medium lacking leucine (-L) to form an arrayed collection of AD-*yqaH** gene fusion mutants. This organized library was then mated with PJ69–4a strains containing either pGBDU-*dnaA* or pGBDU-*spo0A*, or an empty pGBDU plasmid as a negative control. Selective pressure for interacting phenotypes was then applied on media lacking –LUH or –LUA. Diploids that failed to grow on interaction-selective media were considered as potentially expressing an LOI mutant of *yqaH*. Importantly, any particular AD-YqaH*-LOI protein unable to trigger interacting phenotypes in the presence of BD-DnaA while still producing interacting phenotypes when expressed in the presence of BD-Spo0A is defined as a DnaA-specific LOI mutant. The corresponding *yqaH-LOI* genes were retrieved from the initially organized haploid library and the mutations were identified by DNA sequencing. Only mutations resulting from single substitutions were considered.

Ori/Ter ratio determination

The ratios of origin-proximal and terminus-proximal DNA sequences were determined by quantitative PCR (qPCR). ON cultures of *B. subtilis* strains containing pDG148 or pDG148-*yqaH* plasmid derivatives were first diluted to OD_{600} of 0.01 in LB supplemented with kanamycin (5 µg ml^{-1}) and grown at 37 °C up to mid-exponential phase (OD_{600} 0.3–0.4). Then the cultures were secondly diluted at OD_{600} of 0.02 in LB+kanamycin media supplemented with 0.5 mM IPTG and grown again up to an OD_{600} of 0.3–0.4 at 37 °C. Culture samples were collected and mixed with 1/2 volume of sodium azide solution (5 mM final) to stop all metabolic activities prior subjecting them to total lysis. Aliquots of total genomic DNA extracts were kept at −80 °C and were only used once after defrosting. Quantitative real-time PCRs were performed on a Mastercycler ep realplex (Eppendorf) thermocycler device using ABsolute Blue QPCR SYBR Green ROX Mix (ABgene), to amplify specific origin (Ori) or terminus (Ter) proximal sequences. Primers used for sequence amplification were chosen using the Primer3Plus program (http://www.bioinformatics.nl/ cgi-bin/primer3plus/primer3plus.cgi/). Amplification using the ORI pair of primers (oriL3F and oriL3R, Table S2) targeting the 4212889–4211510 region of the *B. subtilis* chromosome yields a 128 bp size product corresponding to sequence at the left side of the origin. The terminus sequence is a 122 bp long fragment obtained from the Ter pair of primers (terR3F and terR3R, Table S2) amplifying the region 2016845–2017711 at the right side of the terminus. The two primer pairs Ori and Ter exhibited ≥95 % amplification efficiency. Data analysis was performed using the software Realplex (Eppendorf) and quantification was done with the ΔΔCt method.

Gene expression analysis by qPCR

To monitor the expression of the DnaA-regulated gene *dnaA*, samples of cultures (generated as described for Ori/Ter ratio measurements) were harvested in exponential growth phase at OD_{600} of 0.3–0.4, and RNA extractions were performed. To quantify the expression of Spo0A-regulated genes *spoIIE* and *spoIIGA*, cells were harvested between stages t_2 and t_3 of sporulation in SM medium. In both cases, a determined volume of culture was mixed with 1/2 volume of sodium azide solution (5 mM final), then collected by centrifugation and subjected to lysis followed by total RNA extraction as described [66]. Total RNA was reverse transcribed and quantitative real-time PCR was performed on cDNA. Primers used for sequence amplification were chosen using Primer3Plus (http://www.bioinformatics.nl/cgi-bin/primer3plus/primer3plus.cgi/) and are detailed in Table S2. The primer pairs exhibited ≥95 % amplification efficiency. Data analysis was performed using the software Realplex (Eppendorf) and the quantification was done with the ΔΔCt method.

(a)
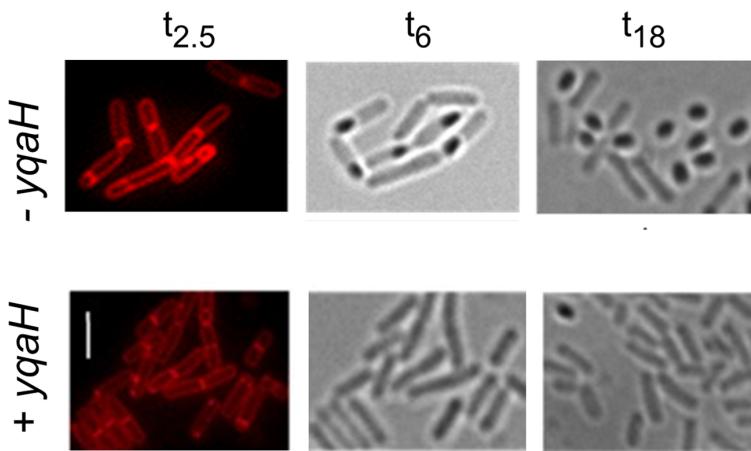
(b)
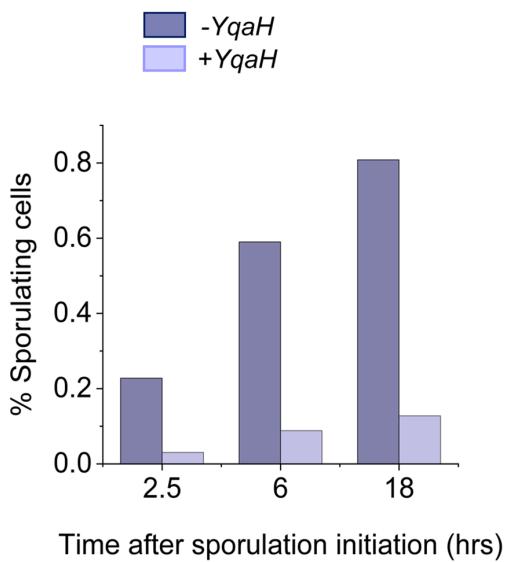
(c)
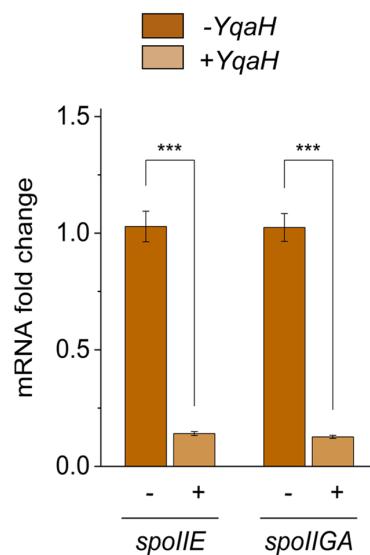
Fig. 3. YqaH triggers sporulation and Spo0A-related phenotypes. (a, b) Overexpression of *yqaH* inhibits sporulation. Cells carrying plasmids pDG148 (control) or pDG148-yqaH were grown in Sterlini-Mandelstam medium in the presence of IPTG (0.5 mM) added at the onset (t_0) of sporulation. Sporulating cells were observed at different times after initiation of sporulation. (a) Snapshot captures of light and fluorescence microscopy at indicated times. Cells were stained with the fluorescent membrane dye FM4-64 (left panel). (b) Sporulating cells were quantified by monitoring asymmetric septa, engulfed forespores and free spores, in the presence (+) or absence (-) of YqaH. Ratios were determined from observation of ≥500 cells over two independent experiments and three biological replicates per experiment. (c) YqaH affects expression of Spo0A-regulated genes. Expression levels of *spoIIE* and *spoIIGA* genes from the Spo0A regulon were monitored by real-time qPCR in the presence (+) or absence (-) of YqaH and expressed as relative expression ratio compared to control (-). Data are presented as mean±SE; $n≥8$ from two independent experiments. ***$P<0.001$ (*t*-test).

Real-time *in vivo* monitoring of *spoIIG* gene expression by luminescence

The promoter of *spoIIG* fused to the firefly luciferase gene *luc* [81] was transferred in the BSBA1 background strains by transformation with total genomic DNA. Cell growth was monitored in a 96-well microplate under agitation at 37 °C using a microplate reader (Biotek Synergy2). Luminescence as well as OD_{600} were recorded every 5 min. Luminescence signals were expressed as relative

luminescence units (RLU) normalized to the bacterial OD. For monitoring of *spoIIG* expression during sporulation, precultures of strains harbouring plasmid pDG148-*yqaH* wild-type and mutated derivatives were first performed in LB supplemented with kanamycin ($10\,\mu g\,ml^{-1}$) over 1 day. Cells from precultures were then inoculated in CH media at very high dilution so they could reach an OD_{600} of 1 after 12 h (ON). Then cells were re-suspended in SM medium supplemented with 0.5 mM IPTG and inoculated in 96-well microplates in the presence of luciferin ($1.4\,mg\,ml^{-1}$). The cultures were incubated at 37 °C under agitation in a plate reader equipped with a photomultiplier for luminometry. RLU and OD_{600} were measured at 5 min intervals.

Fluorescence microscopy

For observation of nucleoids, cells were grown and harvested as described for Ori/Ter measurements, then rinsed in a minimal transparent media, and stained with FM4-64 dye (to stain the bacterial membranes) and DAPI (to stain the nucleoids) prior to being mounted onto 1.2% agarose pads. Fluorescence microscopy was performed on a Leica DMR2A (100× UplanAPO objective with an aperture of 1.35) coupled with a CoolSnap HQ camera (Roper Scientific). System control and image processing were achieved using Metamorph software (Molecular Devices). Counts of cells, spores, foci or nucleoids were determined with the ImageJ software, from at least 500 cells.

Biofilm assay

Production and analysis of air-to-liquid biofilm pellicles were performed as already described [82]. Briefly, strains expressing *yqaH*, wild-type or K17E mutant derivative as well as the control strain were grown in LB to an OD_{600} of 1.0 and inoculated in 12-well culture plates containing 3.5 ml of MSgg media at a starting OD_{600} of 0.1. Cultures were maintained at 28 °C and 70% humidity, with no agitation. After 48 h, wells were filled with MSgg media (slowly added at the edge) to lift the biofilm pellicles up to the top of the wells. The pellicles were then peeled off onto a 2.5 cm diameter circular cover slide. The cover slides with intact biofilm pellicles were mounted on an Attofluor Cell Chamber and stained with the Film Tracer FM 1–43 Green Biofilm dye (Thermo Fisher Scientific). Stained biofilms were observed using a spinning disc confocal microscope [Nikon Eclipse Ti-E coupled with CREST X-Light confocal imager; objectives Nikon CFI Plan Fluor 10×, DIC, 10×/0.3 NA (WD=16 mm); excitation was performed at 470 nm and emission recorded at 505 nm]. Images were processed using IMARIS software (Bitplane). Biofilm images were quantified using the surface function in IMARIS (XTension biofilm) to derive biovolumes [total volume (μm^3) per area (μm^2)], cohesiveness (number of discontinuous components in the area) and mean thickness (μm). Parameters were averaged from eight samples. Pairwise comparisons were performed using the Tukey method (*$P \leq 0.05$, **$P \leq 0.01$, ***$P \leq 0.001$).

Protein extraction and immunodetection

Production of 3Flag-YqaH mutated derivatives was determined from cell lysates of *B. subtilis* followed by immunodetection using the monoclonal antibody anti-FLAG M2 (Sigma). For cell lysates, cells expressing the 3Flag-YqaH derivatives (OD_{600} 0.15) were grown in the presence of IPTG for 1 h and collected. Cells were ressuspended in lysis buffer (10 mM Tris pH 7.7, 200 mM NaCl, 1 mM EDTA) and lysed by sonication. Lysates were first centrifuged at 20 000 *g* for 20 min at 4 °C. The Bradford method was used to estimate the quantity of proteins within soluble fractions prior to loading on a SDS-PAGE 12.5% polyacrylamide gel for electrophoresis separation. To assess YqaH solubility, the remaining supernatant was further subjected to ultra-centrifugation (100 000 *g*, 1 h, at 4 °C), and an equivalent amount of proteins (40 ng, assayed by the Bradford method) from the high-speed soluble phase was again loaded onto the SDS-PAGE gel. Proteins were electrophoretically separated and transferred to PVDF membranes. YqaH was detected using a monoclonal anti-FLAG M2 antibody (F2135; Sigma). An IgG goat secondary antibody (A2304; Sigma) conjugated to peroxidase was used at 1:10 000 to detect the anti-FLAG M2. Protein immunodetection was performed using the Clarity Western ECL kit (Bio-Rad) according to the supplier's indications followed by chemiluminescence detection (ChemiDoc imager; Bio-Rad). Images were analysed with the software Image Lab.

Structure predictions

Secondary structure predictions were performed with the computer server Jpred 3 (http://www.compbio.dundee.ac.uk/www-jpred/) and the 3D structure was predicted using Alphafold [83] (https://alphafold.ebi.ac.uk).

RESULTS

Skin element smORF-encoded YqaH interacts with DnaA and Spo0A

YqaH was originally identified to interact with the replication initiator DnaA in a yeast two-hybrid screen of a *B. subtilis* genomic library [70]. Interestingly, in a subsequent screen targeting the sporulation transcription factor Spo0A, we also identified YqaH as a binding partner (Fig. 1b). Other DnaA-binding proteins such as SirA, Soj, DnaD and YabA exert regulatory functions by binding to different functional domains of DnaA (Fig. 1b, d). We characterized the domain of DnaA able to elicit the interaction phenotypes with YqaH in a yeast two-hybrid binary assay. After testing several protein fragments spanning various DnaA domains, we delineated the C-terminal domain IV as necessary and sufficient for interaction with YqaH (Fig. 1c, d). This 118

(a)

(b)
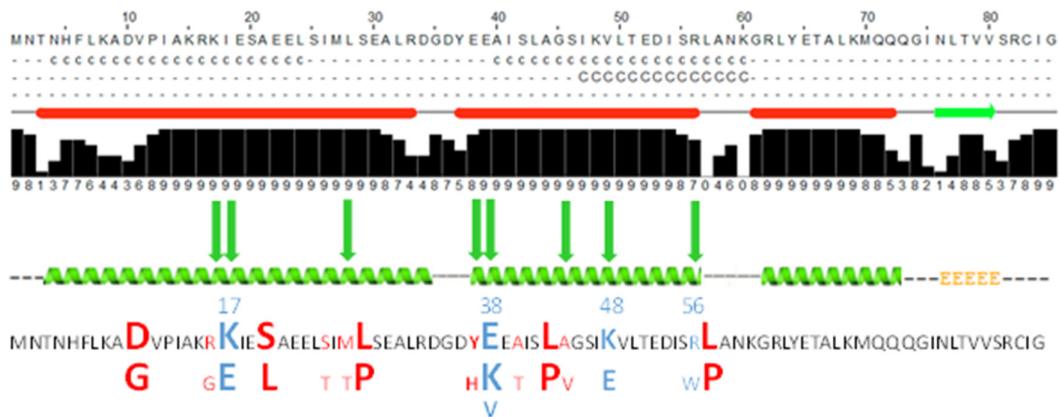
YqaH_LOI		DnaA	Spo0A
	D10G	-	-
	R16G	+/-	+
	K17E	-	+
	S20L	-	-
	S25T	+/-	+/-
	M27T	+/-	+
	L28P	-	-
	Y37H	+/-	+
	E38K	-	+
	E38V	+/-	+
	A40T	+/-	+/-
	L43P	-	-
	A44V	+/-	+
	K48E	-	+
	R56W	+/-	+
	L57P	-	-

(c)
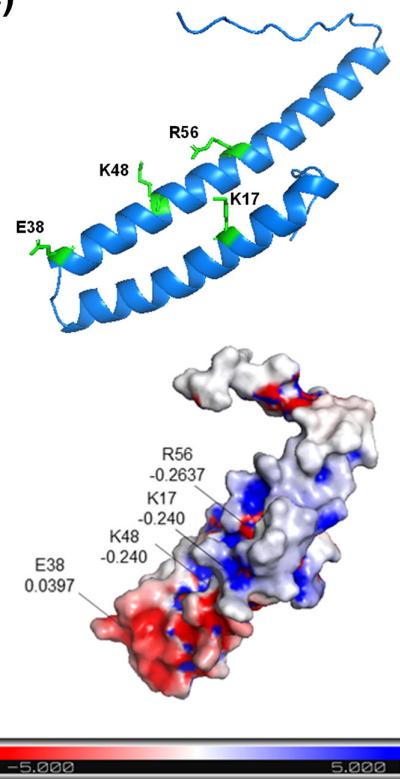
Fig. 4. Mapping of DnaA_LOI mutations in YqaH. (a) The YqaH protein is predicted to fold into three α- helices (http://www.compbio.dundee.ac.uk./www-jpred/). Single-substituted amino acids are highlighted in red and blue, and the nature of the substitutions is indicated beneath. Upper case indicates an LOI phenotype monitored on both –His and –Ade selective media. Lower case indicates that the LOI phenotype has been obtained on the most selective –Ade media only but not on –His media, indicative of a partial loss of interaction. The four mutations highlighted in blue are mapped on the cartoon structure shown in (c). (b) YqaHLOI mutational screen. Amino acid substitutions affecting interaction with DnaA and/or Spo0A are indicated with their associated interaction phenotype. (+) indicates unchanged interaction phenotypes compared to YqaH WT, and characterized by a full ability of diploids to grow on both selective –LUH and –LUA media. (-) refers as a total loss of interaction phenotype leading to absence of growth on both –LUH and –LUA media. (+/-) refers as a partial loss of interaction leading to some growth on –LUH but not –LUA; see also Fig. S1 for additional explanation. (c) Top: mapping of four substituted residues (green sticks) on the cartoon representation of an Alphafold-predicted YqaH structure (per-residue confidence score PLDDT>90) [83], visualized by PyMOL (2.4.1). Bottom: electrostatic surfaces and charge distribution (APBS software package into PyMOL) with ±5 kT e^{-1} electrostatic potential plotted on the solvent-accessible surface. The charge of substituted amino acids is indicated.
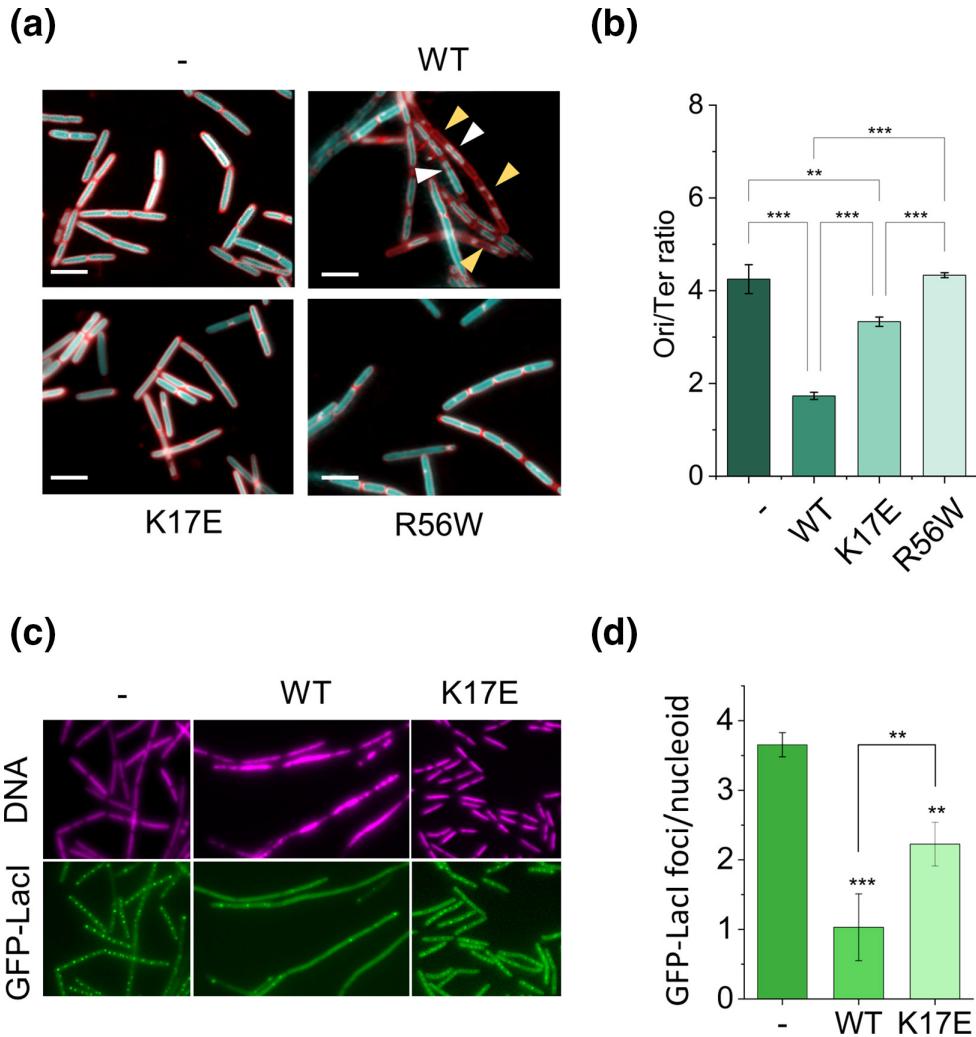
Fig. 5. Restoration of replication initiation defects by YqaH-DnaA_LOI mutation. *B. subtilis* cells carrying either pDG148 (-), pDG148-yqaH (WT), and pDG148-yqaH LOI mutant derivatives K17E or R56W were grown in the presence of IPTG and assessed for various *dnaA*-related phenotypes. (a) Nucleoid morphological phenotypes. Cells were treated with DAPI to reveal nucleoids (false-coloured blue) and with the membrane dye FM4-64 (false coloured red). White and yellow arrows indicate septum-entrapped nucleoids and aberrant condensation and segregation, respectively. Bars, 5 µm. (b–d) Analysis of DnaA-dependent replication initiation phenotypes. (b) Ori/Ter ratio; origin-proximal and terminus proximal DNA sequences were quantified by qPCR. (c) Visualization of origins foci in living cells. Origins are visualized through binding of the GFP-LacI repressor to LacO operator sequences inserted at a proximal location from oriC. (d) Average number of replication origins per cell determined as the number of GFP-LacI foci upon induced conditions in control (-), WT and K17E- mutant derivative of YqaH. Statistical significance is indicated by asterisks (*t*-test; Ori/Ter: *n*=6; dnaA mRNA: *n*=12; *$P<0.05$, **$P<0.01$, ***$P<0.001$.

aa long fragment spans residues 328–446, and carries the signature motif for DnaA binding to dsDNA. This result distinguishes YqaH from the other regulators SirA, Soj, YabA and DnaD that inhibit DnaA binding to *oriC,* through interacting with the central AAA+ATPase domain III (aa 111–328, Fig. 1d). SirA also inhibits DnaA oligomerization by interacting with domain I. The ability of YqaH to interact with two key players of bacterial vegetative growth and transition to sporulation development prompted us to further explore the biological functions of YqaH .

Induction of *yqaH* expression triggers phenotypes similar to those of a DnaA mutant

The interaction of YqaH with DnaA hints at a potential role in replication initiation control. We first investigated the effect of *yqaH* overexpression on cell growth and viability. All *B. subtilis* strains either carrying a plasmid expressing *yqaH* under control of an IPTG-inducible promoter or carrying a control plasmid without the *yqaH* gene were treated under identical conditions. Addition of IPTG at an early exponential stage specifically halted cell growth after 2 h in cells expressing *yqaH* (Fig. 2a). We found that cell viability was affected almost instantly in the presence of *yqaH*, leading to an about 30-fold decrease after 3 h (Fig. 2a). Overexpression of *yqaH* also affects cell morphology, causing significant filamentation (Fig. 2b). A closer examination
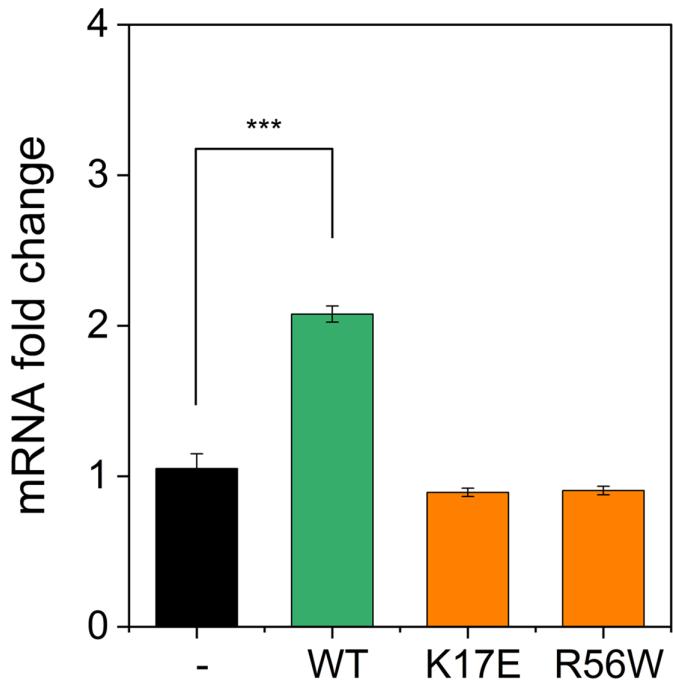
Fig. 6. Effect of YqaH LOI mutants on *dnaA* expression. Cells harbouring either the pDG148, pDG148-yqaH WT or K17E and R56W mutated derivatives were grown in LB in the presence of IPTG. RNAs from exponentially grown cells (OD_{600}~0.3) were extracted and expression levels of the *dnaA* gene were monitored by qPCR in the absence (-) or in the presence of YqaH (WT, K17E, or R56W). Data are presented as mean±SE; *n*=12 from two independent experiments with two biological replicates per experiment. ***$P<0.001$ (*t*-test).

of nucleoids revealed aberrant segregation of chromosomes with both diffused and compacted nucleoids unequally distributed within the filamented cells, as well as a large portion of cells with no DNA. Most importantly, septum-entrapped nucleoids were also observed, evocative of a nucleoid occlusion defect [84]. These observations highlighted that the synthetic overexpression of *yqaH* from a plasmid triggered a large panel of chromosomal disorders evocative of a replication and/or segregation stress, as described previously [67]. Using an epitope-tagged YqaH protein, we showed that YqaH was immuno-detected in cells carrying the IPTG-inducible *yqaH* gene but not in the control, indicating that the chromosomal copy of *yqaH* within the *skin* element remained completely silent under our experimental conditions (Fig. S2).

We then investigated the role of YqaH on DnaA-dependent transcriptional regulation. Among the genes of the DnaA-regulon, DnaA negatively regulates its own expression by binding to the *dnaA* promoter region [53, 55, 85]. We monitored the *dnaA* mRNA levels in the presence or absence of YqaH and showed that expression of *yqaH* led to a 2-fold increase in *dnaA* mRNA, consistent with a regulatory defect (Fig. 2c). Taken together, these results are in agreement with a role of YqaH in counteracting DnaA activity.

Induction of *yqaH* expression impairs sporulation

We investigated the possible role of YqaH in Spo0A functions, by examining the effect of *yqaH* overexpression on sporulation. Cells carrying plasmids with or without the *yqaH* gene were induced into sporulation by the re-suspension method. To prevent an inhibitory effect of YqaH during vegetative growth, *yqaH* gene expression was induced only at the onset of sporulation (t_0) and spore formation was monitored over time. Appearance of asymmetric septa at an early stage ($t_{2.5}$) was imaged by fluorescence microscopy after staining by a red-fluorescent membrane dye, while the engulfed forespore (t_6 and t_{18}) was revealed using bright-field microscopy (Fig. 3a). The counts of spore-forming bacteria were drastically reduced in the presence of YqaH (Fig. 3b). We also examined the effect of *yqaH* overexpression on Spo0A-mediated transcriptional regulation. Among genes under control of Spo0A are *spoIIE*, encoding the protein serine phosphatase SpoIIE, and *spoIIGA*, encoding a pro-σ^E-processing protease SpoIIGA [72]. SpoIIE and SpoIIGA are involved in activation of the alternative sporulation sigma factors σ^F and σ^E in the forespore and mother cell compartments, respectively [86–89]. Examination of their expression levels at the onset of sporulation revealed a significant downregulation (about 7- and 8-fold, respectively) in the presence of *yqaH* (Fig. 3c). Together, these results pointed to a negative effect of YqaH during sporulation, supporting the notion that YqaH could act by inhibiting Spo0A activity.
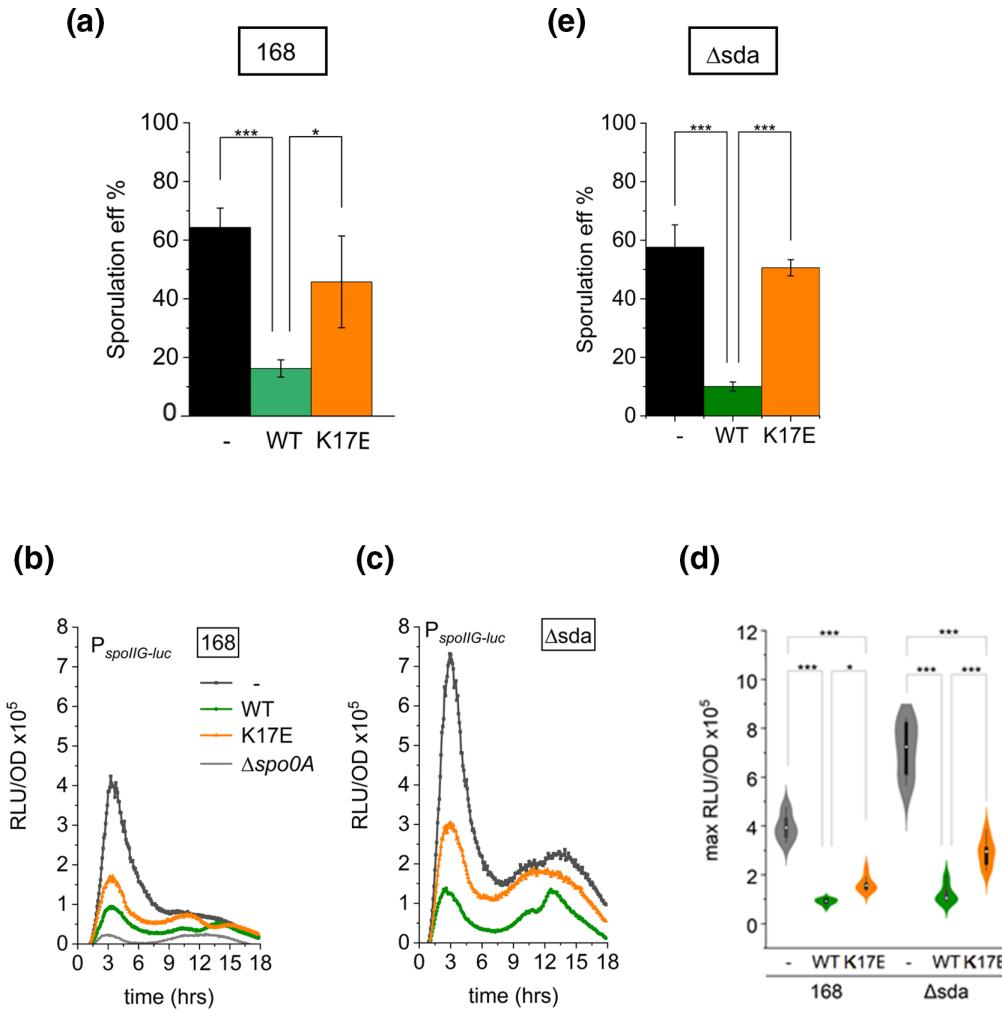
Fig. 7. Effect of the YqaH-K17E mutant on Spo0A activity. (a, e) Sporulation efficiency in *B. subtilis* 168 sda+ and Δsda. Sporulating cells were quantified by monitoring asymmetric septa, engulfed forespores 6 h after sporulation initiation, in the absence (-) or in the presence of YqaH WT and K17E. Ratios were determined from observation of >500 cells over two independent experiments and three biological replicates per experiment. Pairwise comparisons were performed using the Holm–Bonferroni method (*$P \leq 0.05$, **$P \leq 0.01$, ***$P \leq 0.001$). (b–d) Strains carrying a fusion of the spoIIG promoter to the luciferase coding sequence (luc), and harbouring either plasmid pDG148 (black), pDG148-yqaH WT (green) or the K17E mutant derivative (orange), as well as a strain carrying a PspoIIG-luc in a Δspo0A mutant background (grey) were induced to sporulation in SM medium supplemented with 0.5 mM IPTG. Luminescence was recorded in *B. subtilis* 168 (sda+) (b) and Δsda (c) strain backgrounds. (d) Grouped-violin plot comparing the maximum levels of luciferase at 3 h after sporulation initiation.

Functional dissection of YqaH

To further decipher YqaH's mode of action, we searched for YqaH point mutations able to separate its interactions with DnaA and Spo0A. Using a yeast two-hybrid-based assay, we screened an YqaH mutant library for specific LOI phenotypes (Fig. S1). This approach is used to select single amino acid changes in YqaH that selectively disrupt the interaction with only one partner while maintaining proficiency for interaction with the other partner. Such a screening allows the identification of substitutions of residues preferentially located at the protein–protein interface, preserving the global 3D-structure of YqaH, and leading to an LOI phenotype specific for the targeted partner [78–80]. We identified three single-residue substitutions, K17E, E38K and K48E, in YqaH that elicited a complete LOI phenotype with DnaA without affecting interaction with Spo0A (Fig. 4a, b). These three replacements were all charge-changing substitutions (Fig. 4c). Six additional substitutions affecting residues R16G, M27T, Y37H, E38V A44V and R56W were only partially abolishing interaction phenotypes with DnaA (Fig. 4a, b). Two substitutions, S25T and A40T, were found to partially affect both interaction with DnaA and Spo0A, and five substitutions, D10G, S20L, L28P, L43P and L57P, were totally abolishing interaction phenotypes with both DnaA and Spo0A (Fig. 4b). In the latter case, these substitutions are likely to affect the overall integrity of the YqaH 3D-structure. The YqaH protein structure is predicted to fold into two successive alpha helices separated by a helix–turn–helix (HTH) structural motif (Fig. 4a, c). The residues important for

interaction with DnaA localized within the two main helices, presumably involved in a coiled-coil structure (Fig. 4c). Mapping of the charge distribution on the YqaH model shows that the HTH fold is enriched with negatively charged amino acids (Fig. 4c). It is worthy of note that, although several specific DnaA_LOI mutants have been obtained, no substitution that specifically prevented interaction with Spo0A was identified in our screens.

DnaA_LOI mutants of YqaH restore replication and transcriptional regulation defects caused by *yqaH* overexpression

We investigated the effect of two DnaA_LOI mutants of YqaH carrying substitutions K17E or R56W and exhibiting total (K17E) or partial (R56W) LOI with DnaA in our yeast two-hybrid assay (Fig. 4b). We first verified production levels of the YqaH mutant proteins in the cells upon overexpression from the plasmid compared to the wild-type (Fig. S2). The cellular amounts of YqaH-K17E and R56W were similar to that of the WT and remained soluble after clarification by ultracentrifugation at 100 000 g indicating that the presence of amino acid substitutions did not notably affect the protein stability. (Fig. S2A, B). Examination of the nucleoid morphology showed that both substitutions abolished the nucleoid segregation and condensation defects resulting from expression of the wild-type *yqaH* observed in Fig. 2b (Fig. 5a). We further examined the effect of YqaH mutants on replication initiation by quantifying the chromosomal origin-proximal and terminus-proximal sequences (Fig. 5b). The average Ori/Ter ratio was determined by qPCR on genomic DNA harvested from exponentially growing cells as previously described [90]. The Ori/Ter ratio was about 4 in control cells that did not express *yqaH*, indicating that two events of replication initiation have taken place in most cells, in agreement with previous observations under similar experimental conditions [91]. In the presence of *yqaH*, the Ori/Ter ratio dropped below 2, indicating that less than one replication initiation event per cell has taken place on average (Fig. 5b). This suggests that the YqaH protein exerts a negative effect on replication initiation by counteracting DnaA activity. In the presence of YqaH-DnaA_LOI variants, the Ori/Ter ratio in the cell population was restored (Fig. 5b). The average Ori/Ter ratio was similar to that in control cells upon expression of *yqaH-R56W*. However, expression of *yqaH-K17E* restored about 75% of the initiation rate, indicating a partial although significant complementation. This difference between YqaH variants may be due to a differential LOI with DnaA in cells. We decided to analyse further the number of chromosomal origins in individual cells using the YqaH-K17E mutant. Cells carrying a *lacO* repeat array near the replication origin and expressing the GFP-LacI fusion were observed by fluorescence microscopy, in the presence or absence of YqaH (Fig. 5c). In the absence of YqaH, the number of LacI foci per nucleoid was 3.6 on average, in agreement with the Ori/Ter ratio (Fig. 5b). This number dropped to 1 on average upon ovrexpression of *yqaH*, indicating a strong replication deficit. Cells expressing *yqaH* also exhibited expected aberrant nucleoids and segregation defects. Expression of the *yqaH-K17E* mutant partially restored replication defects with an average of GFP-LacI foci of about 2.3 and fully restored nucleoid and cell morphology. Together, these observations indicate that YqaH antagonizes DnaA activity in replication initiation by binding to DnaA.

We also examined the effect of the DnaA_LOI mutants on *dnaA* mRNA abundance. Similarly to Fig. 2c, expression of *yqaH* increased the abundance of *dnaA* mRNA relative to control by 2-fold (Fig. 6). In contrast, *dnaA* mRNA levels detected in strains expressing the *yqaH-K17E* and R56W variants were similar to the level detected in cells expressing *yqaH*-WT (Fig. 6). This indicated that YqaH binding to DnaA also antagonized DnaA activity in transcriptional regulation.

YqaH-mediated inhibition of sporulation and biofilm formation requires interaction with DnaA

Although we did not identify any YqaH mutant that specifically lost interaction with Spo0A (Spo0A_LOI) in our yeast two-hybrid screen, we reasoned that the DnaA_LOI mutant YqaH-K17E, which remains fully proficient for interaction with Spo0A, could still provide a way to investigate a potential effect of YqaH on sporulation phenotypes. Indeed, despite a slightly reduced Ori/Ter ratio, overexpression of *yqaH-K17E* allows normal vegetative cell growth without the DnaA-related chromosome segregation defects (Fig. 5). We compared the sporulation efficiencies of strains expressing *yqaH* wild-type or the K17E variant. The percentage of cells with a polar septum or engulfing spore was determined by microscopy at t_6 (i.e stage VI, referred as the spore maturation stage). Surprisingly, we found that YqaH-K17E completely restored the sporulation defect mediated by YqaH WT (Fig. 7a) suggesting that the interaction with DnaA could be also responsible for loss of the sporulation phenotype. To further investigate the potential role of YqaH in Spo0A-related processes, we also examined its effect on biofilm formation (Fig. S3). We observed that the production of biofilm pellicles at the air–liquid medium interface was impaired in strains expressing *yqaH*, leading to a loss of biomass and cohesion. Damaged biofilm pellicles were not observed in cells expressing the DnaA_LOI mutant YqaH-K17E (Fig. S3A, B). As *yqaH* expression also affects chromosome segregation and vegetative growth, this finding suggests an indirect role of DnaA during biofilm formation.

The sporulation inhibitor Sda is not responsible for YqaH–mediated defects in sporulation

In *B. subtilis*, most of the DnaA-mediated transcriptional regulation of sporulation genes is indirect and mediated by the protein Sda, as evidenced by genome-wide expression analysis [55]. The Sda protein exerts control over sporulation by inhibiting the phosphorylation activity of KinA, required to activate the sporulation regulator Spo0A [37, 55]. We investigated whether Sda played a role in the YqaH-dependent defect in sporulation by examining the expression of the Spo0A-driven promoter P$_{spoIIG}$

fused with the firefly luciferase reporter gene (*luc*), in the presence or absence of *sda* (Fig. 7b–d). In the absence of YqaH, the expression of P$_{spoIIG-luc}$ increased with time to reach a maximum 3 h after induction of sporulation in both *sda+* and *Δsda* backgrounds. A higher expression level was observed in the *Δsda* strain, in agreement with increased levels of Spo0A-P [92] (Fig. 7b–d). Expression of *yqaH* led to a similarly strong reduction of luminescence signal in both strains, illustrative of an *spoIIG* expression decrease (Fig. 7b–d). By comparison, *spoIIG* expression was abolished in the absence of *spo0A*, as already described [89, 93](Fig. 7b). This indicates that in our experimental condition, the overexpression of *yqaH* is not sufficient to completely counteract the activity of Spo0A. This observation is also corroborated by the strong reduction of sporulation efficiency in both *sda+* and *Δsda* strains (Fig. 7a and e). These results pointed to an *sda*-independent inhibition of sporulation mediated by YqaH. However, the decrease of *spoIIG* expression caused by YqaH WT was only partly compensated for by the DnaA_LOI YqaH-K17E mutant, suggesting that interaction of YqaH with DnaA may have a moderate role in the inhibition of Spo0A activity. Yet, the K17E mutation fully abolished the YqaH-dependent sporulation defect in *sda+* and *Δsda* strains, as measured by the ratio of cells containing asymmetric septa or engulfed forespores 6 h after initiation of sporulation (Fig. 7a and e). Together, these results indicated that Sda was not involved in the DnaA-mediated response to sporulation and suggested a combined role of DnaA and Spo0A in YqaH-mediated sporulation phenotypes.

DISCUSSION

Our study sheds light on some of the mechanisms of action of YqaH, a small protein with growth inhibition activities encoded by the *B. subtilis skin* element. By physically interacting with two master regulators DnaA and Spo0A, YqaH is a multifunctional small peptide, with the potential to act on two key cellular processes. YqaH is able to counteract DnaA, which is essential during vegetative growth as a replication initiator and transcriptional factor. YqaH also interfers with Spo0A, which is an essential regulator of lifestyle transitions in response to changes in environmental conditions, including the transition from vegetative growth to sporulation.

In *Bacillus*, several regulatory proteins inhibit DnaA by targeting different functional domains of the protein. In cells committed to sporulation, the protein SirA prevents DnaA from binding to the replication origin *oriC* by interacting with its structural domains I and III [94]. During vegetative growth, the regulatory protein YabA interacts with DnaA during most of the cell cycle [78, 90, 95]. YabA as well as the primosomal protein DnaD affect DnaA cooperative binding to *oriC* by interacting with DnaA structural domain III [57, 85]. Finally, the ATPase protein Soj negatively regulates DnaA by also interacting with the structural domain III, preventing oligomerization [96]. Our results indicate that YqaH controls DnaA activity by a mode distinct from the other known regulators, specifically by contacting the structural domain IV responsible for binding of the DnaA-binding-sites (DnaA-boxes) on the *Bacillus* genome [97].

B. subtilis cells overexpressing *yqaH* exhibited various DnaA-related phenotypes that spanned from a general growth defect, aberrant nucleoid morphologies, impaired replication initiation and loss of transcriptional control. These cells also exhibited Spo0A-related phenotypes such as a dramatic reduction of sporulation efficiency, an inhibition of Spo0A-driven gene expression and a strong decrease in biofilm formation. These observations are in agreement with a role of YqaH in counteracting both DnaA and Spo0A activities during vegetative growth and sporulation. However, it is well documented that initiation of sporulation is closely coupled to the cell cycle and DNA replication to ensure it occurs only in cells containing two fully replicated chromosomes [40]. The intricate relationship between DNA replication and sporulation makes it difficult to separate the DnaA-related phenotypes from those linked to Spo0A. By using YqaH single-point mutants unable to interact with DnaA but proficient for interaction with Spo0A, we identified a mutational pattern on YqaH and confirmed the direct involvement of YqaH in various DnaA-related phenotypes, validating that LOI caused loss of function in *Bacillus*. In our yeast two-hybrid screens, we did not obtain YqaH Spo0A_LOI mutants. Yet, by using YqaH DnaA_LOI mutants, we revealed that DnaA also played a part in sporulation and biofilm formation.

In *B. subtilis*, many genes regulated by DnaA are involved in sporulation and biofilm formation, illustrating the complexity of regulatory circuits that control lifestyle transitions [55]. However, most of the effect of DnaA on gene expression is indirect and could be attributed to its transcriptional activation of the sporulation checkpoint gene *sda* [55]. We showed that Sda was not involved in the sporulation phenotypes triggered by YqaH, as cells exhibited similar sporulation defects in the presence or absence of Sda. Interestingly, the YqaH-K17E DnaA_LOI mutant separated the observed Spo0A-related phenotypes. Indeed, whereas overexpression of the *yqaH-K17E* mutant enabled total recovery of sporulation efficiency, it did not fully restore the activity of the Spo0A-dependent promoter P$_{spoIIG}$. This finding suggests that YqaH may partially or transiently antagonize Spo0A activity. Further investigation is necessary to fully characterize the interaction of YqaH with Spo0A.

Defective prophages and integrated elements account for a large fraction of bacterial genomes and may contribute to gene diversity, bacterial adaptation and fitness [98, 99]. The integration and excision of prophages and prophage-like elements within genes involved in sporulation are described as a phage regulation switch following the co-evolution between a phage and its spore-forming bacterium [100, 101]. In *B. subtilis*, the *skin* element is under tight control by the *skin* repressor protein SknR. Its excision is restricted to the terminal mother cell at a late stage of sporulation after the completion of engulfment of the pre-spore, leading

to reconstitution of the late sigma factor *sigK*. In *Clostridium difficile*, a smaller *skin*-like element *skin^{Cd}* was found to interrupt the *sigK* gene. Similarly to *B. subtilis*, the excision of *skin^{Cd}* occurs in the mother cell during sporulation and reconstitutes an integral *sigK* [102]. In *C. difficile*, a *skin^{Cd}*-less strain of exhibits a strong sporulation defect [102, 103]. Other bacilli prophage elements inserted into sporulation-related genes have been described. The SPβ prophage of *B. subtilis* disrupts the *spsM* gene, coding for a polysaccharide synthase. The functional SpsM resulting from expression of *spsM* after excision of SPβ in the sporulating mother cell was found to participate in the formation of the exosporium-like structure on the mature spores [104].

Here we validated the biological role of a small protein encoded by the *skin* prophage-like element of *B. subtilis* in negatively interfering with a broad range of cellular processes by counteracting two master regulators, DnaA and Spo0A. The excision of *skin* in the mother cell, potentially leading to the expression of YqaH, could be also part of a mechanism to improve the proper orchestration of forespore development. However, the significance of counteracting DnaA activity in the mother cell at a late stage of sporulation remains to be understood. In the non-spore-forming Gram-negative bacterium *E. coli*, a small protein, YfdR, encoded by a cryptic prophage, CPS-53, was found to bind to DnaA and to play a role in inhibiting replication initiation *in vitro* [105]. In *B. subtilis*, analysis of the occurrence of *skin* excision in the absence of the site-specific recombinase CisA suggested that such a rearrangement can occur by a RecA-dependent homologous recombination process, although at a very low frequency [106]. Whether the *skin* element could be excised in vegetative cells of *B. subtilis* is not documented. However, we postulate that the expression of *yqaH* could also be part of a mechanism to prevent cell growth and the formation of *skin*-less spores. YqaH homologues are present in integrated prophages of other Gram-positive bacteria of the genera *Bacillus* and *Staphylococcus*, as well as in the Gram-negative bacteria *Delftia acidirovans*, suggesting that YqaH could confer a beneficial advantage in other hosts under conditions other than sporulation.

Conflicts of interest
The authors declare that the research was conducted in the absence of any commercial or financial relationships that could be construed as a potential conflict of interest.

References

1. **Albuquerque JP, Tobias-Santos V, Rodrigues AC, Mury FB, da Fonseca RN**. small ORFs: a new class of essential genes for development. *Genet Mol Biol* 2015;38:278–283.

2. **Couso J-P, Patraquim P**. Classification and function of small open reading frames. *Nat Rev Mol Cell Biol* 2017;18:575–589.

3. **Hellens RP, Brown CM, Chisnall MAW, Waterhouse PM, Macknight RC**. The emerging world of small ORFs. *Trends Plant Sci* 2016;21:317–328.

4. **Samayoa J, Yildiz FH, Karplus K**. Identification of prokaryotic small proteins using a comparative genomic approach. *Bioinformatics* 2011;27:1765–1771.

5. **Storz G, Wolf YI, Ramamurthi KS**. Small proteins can no longer be ignored. *Annu Rev Biochem* 2014;83:753–777.

6. **Chu Q, Ma J, Saghatelian A**. Identification and characterization of sORF-encoded polypeptides. *Crit Rev Biochem Mol Biol* 2015;50:134–141.

7. **He C, Jia C, Zhang Y, Xu P**. Enrichment-based proteogenomics identifies microproteins, missing proteins, and novel smORFs in *Saccharomyces cerevisiae*. *J Proteome Res* 2018;17:2335–2344.

8. **Makarewich CA, Olson EN**. Mining for Micropeptides. *Trends Cell Biol* 2017;27:685–696.

9. **Straub D, Wenkel S**. Cross-species genome-wide identification of evolutionary conserved microproteins. *Genome Biol Evol* 2017;9:777–789.

10. **VanOrsdel CE, Kelly JP, Burke BN, Lein CD, Oufiero CE, et al.** Identifying new small proteins in *Escherichia coli*. *Proteomics* 2018;18:e1700064.

11. **Saghatelian A, Couso JP**. Discovery and characterization of smORF-encoded bioactive polypeptides. *Nat Chem Biol* 2015;11:909–916.

12. **Staudt A-C, Wenkel S**. Regulation of protein function by "micro-Proteins." *EMBO Rep* 2011;12:35–42.

13. **Dolde U, Rodrigues V, Straub D, Bhati KK, Choi S, et al.** Synthetic microproteins: versatile tools for posttranslational regulation of target proteins. *Plant Physiol* 2018;176:3136–3145.

14. **Graeff M, Wenkel S**. Regulation of protein function by interfering protein species. *Biomol Concepts* 2012;3:71–78.

15. **Zanet J, Benrabah E, Li T, Pélissier-Monier A, Chanut-Delalande H, et al.** Pri sORF peptides induce selective proteasome-mediated protein processing. *Science* 2015;349:1356–1358.

16. **Slavoff SA, Mitchell AJ, Schwaid AG, Cabili MN, Ma J, et al.** Peptidomic discovery of short open reading frame-encoded peptides in human cells. *Nat Chem Biol* 2013;9:59–64.

17. **Slavoff SA, Heo J, Budnik BA, Hanakahi LA, Saghatelian A**. A human short open reading frame (sORF)-encoded polypeptide that stimulates DNA end joining. *J Biol Chem* 2014;289:10950–10957.

18. **Erpf PE, Fraser JA**. The long history of the diverse roles of short ORFs: sPEPs in fungi. *Proteomics* 2018;18:e1700219.

19. **An X, Zhang C, Sclafani RA, Seligman P, Huang M**. The late-annotated small ORF LSO1 is a target gene of the iron regulon of Saccharomyces cerevisiae. *Microbiologyopen* 2015;4:941–951.

20. **Chabes A, Domkin V, Thelander L**. Yeast Sml1, a protein inhibitor of ribonucleotide reductase. *J Biol Chem* 1999;274:36679–36683.

21. Lee YD, Wang J, Stubbe J, Elledge SJ. Dif1 is a DNA-damage-regulated facilitator of nuclear import for ribonucleotide reductase. *Mol Cell* 2008;32:70–80.

22. Kastenmayer JP, Ni L, Chu A, Kitchen LE, Au W-C, *et al*. Functional genomics of genes with small open reading frames (sORFs) in *S. cerevisiae*. *Genome Res* 2006;16:365–373.

23. Friedman RC, Kalkhof S, Doppelt-Azeroual O, Mueller SA, Chovancová M, *et al*. Common and phylogenetically widespread coding for peptides by bacterial small RNAs. *BMC Genomics* 2017;18:553.

24. Miravet-Verde S, Ferrar T, Espadas-García G, Mazzolini R, Gharrab A, *et al*. Unraveling the hidden universe of small proteins in bacterial genomes. *Mol Syst Biol* 2019;15:e8290.

25. Yang X, Jensen SI, Wulff T, Harrison SJ, Long KS. Identification and validation of novel small proteins in *Pseudomonas putida*. *Environ Microbiol Rep* 2016;8:966–974.

26. Zuber P. A peptide profile of the *Bacillus subtilis* genome. *Peptides* 2001;22:1555–1577.

27. Ha U-H, Kim J, Badrane H, Jia J, Baker HV, *et al*. An *in vivo* inducible gene of Pseudomonas aeruginosa encodes an anti-ExsA to suppress the type III secretion system. *Mol Microbiol* 2004;54:307–320.

28. Wu W, Jin S. PtrB of *Pseudomonas aeruginosa* suppresses the type III secretion system under the stress of DNA damage. *J Bacteriol* 2005;187:6058–6068.

29. Lloyd CR, Park S, Fei J, Vanderpool CK. The small protein SgrT controls transport activity of the glucose-specific phosphotransferase system. *J Bacteriol* 2017;199:e00869-16.

30. Ebmeier SE, Tan IS, Clapham KR, Ramamurthi KS. Small proteins link coat and cortex assembly during sporulation in Bacillus subtilis. *Mol Microbiol* 2012;84:682–696.

31. Handler AA, Lim JE, Losick R. Peptide inhibitor of cytokinesis during sporulation in *Bacillus subtilis*. *Mol Microbiol* 2008;68:588–599.

32. Schmalisch M, Maiques E, Nikolov L, Camp AH, Chevreux B, *et al*. Small genes under sporulation control in the *Bacillus subtilis* genome. *J Bacteriol* 2010;192:5402–5412.

33. Araújo-Bazán L, Huecas S, Valle J, Andreu D, Andreu JM. Synthetic developmental regulator MciZ targets FtsZ across *Bacillus* species and inhibits bacterial division. *Mol Microbiol* 2019;111:965–980.

34. Bisson-Filho AW, Discola KF, Castellen P, Blasios V, Martins A, *et al*. FtsZ filament capping by MciZ, a developmental regulator of bacterial division. *Proc Natl Acad Sci U S A* 2015;112:E2130–8.

35. Moeller R, Setlow P, Horneck G, Berger T, Reitz G, *et al*. Roles of the major, small, acid-soluble spore proteins and spore-specific and universal DNA repair mechanisms in resistance of *Bacillus subtilis* spores to ionizing radiation from X rays and high-energy charged-particle bombardment. *J Bacteriol* 2008;190:1134–1140.

36. Setlow P. I will survive: DNA protection in bacterial spores. *Trends Microbiol* 2007;15:172–180.

37. Burkholder WF, Kurtser I, Grossman AD. Replication initiation proteins regulate a developmental checkpoint in *Bacillus subtilis*. *Cell* 2001;104:269–279.

38. Cunningham KA, Burkholder WF. The histidine kinase inhibitor Sda binds near the site of autophosphorylation and may sterically hinder autophosphorylation and phosphotransfer to Spo0F. *Mol Microbiol* 2009;71:659–677.

39. Rowland SL, Burkholder WF, Cunningham KA, Maciejewski MW, Grossman AD, *et al*. Structure and mechanism of action of Sda, an inhibitor of the Histidine Kinases that regulate initiation of sporulation in *Bacillus subtilis*. *Molecular Cell* 2004;13:689–701.

40. Veening J-W, Murray H, Errington J. A mechanism for cell cycle regulation of sporulation initiation in *Bacillus subtilis*. *Genes Dev* 2009;23:1959–1970.

41. Duval M, Cossart P. Small bacterial and phagic proteins: an updated view on a rapidly moving field. *Curr Opin Microbiol* 2017;39:81–88.

42. Liu B, Shadrin A, Sheppard C, Mekler V, Xu Y, *et al*. A bacteriophage transcription regulator inhibits bacterial transcription initiation by σ-factor displacement. *Nucleic Acids Res* 2014a;42:4294–4305.

43. Liu B, Shadrin A, Sheppard C, Mekler V, Xu Y, *et al*. The sabotage of the bacterial transcription machinery by a small bacteriophage protein. *Bacteriophage* 2014b;4:e28520.

44. Nechaev S, Imburgio D, Severinov K. Purification and characterization of bacteriophage-encoded inhibitors of host RNA polymerase: T-odd phage gp2-like proteins. *Methods Enzymol* 2003;370:212–225.

45. Savalia D, Robins W, Nechaev S, Molineux I, Severinov K. The role of the T7 Gp2 inhibitor of host RNA polymerase in phage development. *J Mol Biol* 2010;402:118–126.

46. Hood IV, Berger JM. Viral hijacking of a replicative helicase loader and its implications for helicase loading control and phage replication. *Elife* 2016;5:e14158.

47. Liu J, Dehbi M, Moeck G, Arhin F, Bauda P, *et al*. Antimicrobial drug discovery through bacteriophage genomics. *Nat Biotechnol* 2004;22:185–191.

48. Hwang DS, Kornberg A. Opening of the replication origin of *Escherichia coli* by DnaA protein with protein HU or IHF. *J Biol Chem* 1992;267:23083–23086.

49. Leonard AC, Grimwade JE. Regulation of DnaA assembly and activity: taking directions from the genome. *Annu Rev Microbiol* 2011;65:19–35.

50. Mott ML, Berger JM. DNA replication initiation: mechanisms and regulation in bacteria. *Nat Rev Microbiol* 2007;5:343–354.

51. Ozaki S, Katayama T. DnaA structure, function, and dynamics in the initiation at the chromosomal origin. *Plasmid* 2009;62:71–82.

52. Messer W. The bacterial replication initiator DnaA. DnaA and oriC, the bacterial mode to initiate DNA replication. *FEMS Microbiol Rev* 2002;26:355–374.

53. Goranov AI, Katz L, Breier AM, Burge CB, Grossman AD. A transcriptional response to replication status mediated by the conserved bacterial replication protein DnaA. *Proc Natl Acad Sci USA* 2005;102:12932–12937.

54. Messer W, Weigel C. DnaA as a transcription regulator. *Meth Enzymol* 2003;370:338–349.

55. Washington TA, Smith JL, Grossman AD. Genetic networks controlled by the bacterial replication initiator and transcription factor DnaA in *Bacillus subtilis*. *Mol Microbiol* 2017;106:109–128.

56. Katayama T, Ozaki S, Keyamura K, Fujimitsu K. Regulation of the replication cycle: conserved and diverse regulatory systems for DnaA and oriC. *Nat Rev Microbiol* 2010;8:163–170.

57. Scholefield G, Murray H. YabA and DnaD inhibit helix assembly of the DNA replication initiation protein DnaA. *Mol Microbiol* 2013;90:147–159.

58. Felicori L, Jameson KH, Roblin P, Fogg MJ, Garcia-Garcia T, *et al*. Tetramerization and interdomain flexibility of the replication initiation controller YabA enables simultaneous binding to multiple partners. *Nucleic Acids Res* 2016a;44:449–463.

59. Jameson K, Wilkinson A. Control of Initiation of DNA Replication in *Bacillus subtilis* and *Escherichia coli*. *Genes* 2017;8:22.

60. Katayama T, Kasho K, Kawakami H. The DnaA Cycle in *Escherichia coli*: activation, function and inactivation of the initiator protein. *Front Microbiol* 2017;8:2496.

61. Riber L, Frimodt-Møller J, Charbon G, Løbner-Olesen A. Multiple DNA binding proteins contribute to timing of chromosome replication in *E. coli*. *Front Mol Biosci* 2016;3:29.

62. Skarstad K, Katayama T. Regulating DNA replication in bacteria. *Cold Spring Harb Perspect Biol* 2013;5:a012922.

63. Bonilla CY, Grossman AD. The primosomal protein DnaD inhibits cooperative DNA binding by the replication initiator DnaA in *Bacillus subtilis*. *J Bacteriol* 2012;194:5110–5117.

64. Martin E, Williams HEL, Pitoulias M, Stevens D, Winterhalter C, *et al*. DNA replication initiation in *Bacillus subtilis*: structural and functional characterization of the essential DnaA-DnaD interaction. *Nucleic Acids Res* 2019;47:2101–2112.

65. Murray H, Errington J. Dynamic control of the DNA replication initiation protein DnaA by Soj/ParA. *Cell* 2008;135:74–84.

66. Nicolas P, Mäder U, Dervyn E, Rochat T, Leduc A, *et al*. Condition-dependent transcriptome reveals high-level regulatory architecture in *Bacillus subtilis*. *Science* 2012;335:1103–1106.

67. Kimura T, Amaya Y, Kobayashi K, Ogasawara N, Sato T. Repression of sigK intervening (skin) element gene expression by the CI-like protein SknR and effect of SknR depletion on growth of Bacillus subtilis cells. *J Bacteriol* 2010;192:6209–6216.

68. Kunkel B, Losick R, Stragier P. The *Bacillus subtilis* gene for the development transcription factor sigma K is generated by excision of a dispensable DNA element containing a sporulation recombinase gene. *Genes Dev* 1990;4:525–535.

69. Marchadier E, Carballido-López R, Brinster S, Fabret C, Mervelet P, *et al*. An expanded protein-protein interaction network in *Bacillus subtilis* reveals a group of hubs: exploration by an integrative approach. *Proteomics* 2011;11:2981–2991.

70. Noirot-Gros M-F, Dervyn E, Wu LJ, Mervelet P, Errington J, *et al*. An expanded view of bacterial DNA replication. *Proc Natl Acad Sci U S A* 2002;99:8342–8347.

71. Dubnau EJ, Carabetta VJ, Tanner AW, Miras M, Diethmaier C, *et al*. A protein complex supports the production of Spo0A-P and plays additional roles for biofilms and the K-state in *Bacillus subtilis*. *Mol Microbiol* 2016;101:606–624.

72. Molle V, Fujita M, Jensen ST, Eichenberger P, González-Pastor JE, *et al*. The Spo0A regulon of *Bacillus subtilis*. *Mol Microbiol* 2003;50:1683–1701.

73. James P, Halladay J, Craig EA. Genomic libraries and a host strain designed for highly efficient two-hybrid selection in yeast. *Genetics* 1996;144:1425–1436.

74. Durfee T, Nelson R, Baldwin S, Plunkett G 3rd, Burland V, *et al*. The complete genome sequence of *Escherichia coli* DH10B: insights into the biology of a laboratory workhorse. *J Bacteriol* 2008;190:2597–2606.

75. Stragier P, Bonamy C, Karmazyn-Campelli C. Processing of a sporulation sigma factor in *Bacillus subtilis*: How morphological structure could control gene expression. *Cell* 1988;52:697–704.

76. Weir M, Keeney JB. PCR mutagenesis and gap repair in yeast. *Methods Mol Biol* 2014;1205:29–35.

77. Sterlini JM, Mandelstam J. Commitment to sporulation in *Bacillus subtilis* and its relationship to development of actinomycin resistance. *Biochem J* 1969;113:29–37.

78. Noirot-Gros M-F, Velten M, Yoshimura M, McGovern S, Morimoto T, *et al*. Functional dissection of YabA, a negative regulator of DNA replication initiation in *Bacillus subtilis*. *Proc Natl Acad Sci U S A* 2006;103:2368–2373.

79. Natrajan G, Noirot-Gros MF, Zawilak-Pawlik A, Kapp U, Terradot L. The structure of a DnaA/HobA complex from *Helicobacter pylori* provides insight into regulation of DNA replication in bacteria. *Proc Natl Acad Sci U S A* 2009;106:21115–21120.

80. Quevillon-Cheruel S, Campo N, Mirouze N, Mortier-Barrière I, Brooks MA, *et al*. Structure-function analysis of pneumococcal DprA protein reveals that dimerization is crucial for loading RecA recombinase onto DNA during transformation. *Proc Natl Acad Sci U S A* 2012;109:E2466–75.

81. Mirouze N, Prepiak P, Dubnau D. Fluctuations in spo0A transcription control rare developmental transitions in *Bacillus subtilis*. *PLoS Genet* 2011;7:e1002048.

82. García García T, Ventroux M, Derouiche A, Bidnenko V, Correia Santos S, *et al*. Phosphorylation of the *Bacillus subtilis* replication controller YabA plays a role in regulation of sporulation and biofilm formation. *Front Microbiol* 2018;9:486.

83. Jumper J, Evans R, Pritzel A, Green T, Figurnov M, *et al*. Highly accurate protein structure prediction with AlphaFold. *Nature* 2021;596:583–589.

84. Wu LJ, Errington J. Nucleoid occlusion and bacterial cell division. *Nat Rev Microbiol* 2011;10:8–12.

85. Merrikh H, Grossman AD. Control of the replication initiator DnaA by an anti-cooperativity factor. *Mol Microbiol* 2011;82:434–446.

86. Baldus JM, Green BD, Youngman P, Moran CP Jr. Phosphorylation of *Bacillus subtilis* transcription factor Spo0A stimulates transcription from the spoIIG promoter by enhancing binding to weak 0A boxes. *J Bacteriol* 1994;176:296–306.

87. Bradshaw N, Levdikov VM, Zimanyi CM, Gaudet R, Wilkinson AJ, *et al*. A widespread family of serine/threonine protein phosphatases shares a common regulatory switch with proteasomal proteases. *Elife* 2017;6:e26111.

88. Errington J, Wu LJ. Cell cycle machinery in *Bacillus subtilis*. *Subcell Biochem* 2017;84:67–101.

89. Fujita M, González-Pastor JE, Losick R. High- and low-threshold genes in the Spo0A regulon of *Bacillus subtilis*. *J Bacteriol* 2005;187:1357–1368.

90. Soufo CD, Soufo HJD, Noirot-Gros M-F, Steindorf A, Noirot P, *et al*. Cell-cycle-dependent spatial sequestration of the DnaA replication initiator protein in *Bacillus subtilis*. *Dev Cell* 2008;15:935–941.

91. Murray H, Koh A. Multiple regulatory systems coordinate DNA replication with cell growth in *Bacillus subtilis*. *PLoS Genet* 2014;10:e1004731.

92. Hoover SE, Xu W, Xiao W, Burkholder WF. Changes in DnaA-dependent gene expression contribute to the transcriptional and developmental response of *Bacillus subtilis* to manganese limitation in Luria-Bertani medium. *J Bacteriol* 2010;192:3915–3924.

93. Seredick SD, Spiegelman GB. The *Bacillus subtilis* response regulator Spo0A stimulates sigmaA-dependent transcription prior to the major energetic barrier. *J Biol Chem* 2004;279:17397–17403.

94. Jameson KH, Rostami N, Fogg MJ, Turkenburg JP, Grahl A, *et al*. Structure and interactions of the *Bacillus subtilis* sporulation inhibitor of DNA replication, SirA, with domain I of DnaA. *Mol Microbiol* 2014;93:975–991.

95. Felicori L, Jameson KH, Roblin P, Fogg MJ, Garcia-Garcia T, *et al*. Tetramerization and interdomain flexibility of the replication initiation controller YabA enables simultaneous binding to multiple partners. *Nucleic Acids Res* 2016b;44:449–463.

96. Scholefield G, Veening J-W, Murray H. DnaA and ORC: more than DNA replication initiators. *Trends Cell Biol* 2011;21:188–194.

97. Fujikawa N, Kurumizaka H, Nureki O, Terada T, Shirouzu M, *et al*. Structural basis of replication origin recognition by the DnaA protein. *Nucleic Acids Res* 2003;31:2077–2086.

98. Bobay L-M, Touchon M, Rocha EPC. Pervasive domestication of defective prophages by bacteria. *Proc Natl Acad Sci U S A* 2014;111:12127–12132.

99. Casjens S. Prophages and bacterial genomics: what have we learned so far? *Mol Microbiol* 2003;49:277–300.

100. Dragoš A, Priyadarshini B, Hasan Z, Strube ML, Kempen PJ, *et al*. Pervasive prophage recombination occurs during evolution of spore-forming Bacilli. *ISME J* 2021;15:1344–1358.

101. Feiner R, Argov T, Rabinovich L, Sigal N, Borovok I, *et al*. A new perspective on lysogeny: prophages as active regulatory switches of bacteria. *Nat Rev Microbiol* 2015;13:641–650.

102. Haraldsen JD, Sonenshein AL. Efficient sporulation in Clostridium difficile requires disruption of the σK gene. *Mol Microbiol* 2003;48:811–821.

103. Serrano M, Kint N, Pereira FC, Saujet L, Boudry P, *et al*. A recombination directionality factor controls the cell type-specific activation of σK and the fidelity of spore development in Clostridium difficile. *PLoS Genet* 2016;12:e1006312.

104. Abe K, Kawano Y, Iwamoto K, Arai K, Maruyama Y, *et al.* Developmentally-regulated excision of the SPβ prophage reconstitutes a gene required for spore envelope maturation in *Bacillus subtilis*. *PLoS Genet* 2014;10:e1004636.

105. Noguchi Y, Katayama T. The *Escherichia coli* cryptic prophage protein YfdR binds to DnaA and initiation of chromosomal replication is inhibited by overexpression of the gene cluster yfdQ-yfdR-yfdS-yfdT. *Front Microbiol* 2016;7:239.

106. Sato T, Harada K, Kobayashi Y. Analysis of suppressor mutations of spoIVCA mutations: occurrence of DNA rearrangement in the absence of site-specific DNA recombinase SpoIVCA in *Bacillus subtilis*. *J Bacteriol* 1996;178:3380–3383.

Edited by: W. van Schaik and F. M. Commichau